



Article

# Additive Manufacturing of Lightweight Gypsum and Expanded Polystyrene Granulate Composite

Girls Bumanis <sup>1</sup>, Alise Sapata <sup>2</sup>, Maris Sinka <sup>2,\*</sup>, Ella Spurina <sup>2</sup> and Diana Bajare <sup>1</sup>

<sup>1</sup> Department of Building Materials and Products, Riga Technical University, LV-1048 Riga, Latvia; girls.bumanis@rtu.lv (G.B.); diana.bajare@rtu.lv (D.B.)

<sup>2</sup> 3D Concrete Printing Laboratory, Institute of Materials and Structures, Riga Technical University, 1 Paula Valdena Street, LV-1048 Riga, Latvia; alise.sapata@rtu.lv (A.S.); ella.spurina\_1@rtu.lv (E.S.)

\* Correspondence: maris.sinka@rtu.lv

**Abstract:** Additive manufacturing by 3D printing has emerged as a promising construction method offering numerous advantages, including reduced material usage and construction waste, faster build times, and optimized architectural forms. One area where 3D printing's potential remains largely unexplored is in combination with lightweight materials, especially lightweight gypsum. This research paper explores the potential of combining 3D printing technology with lightweight gypsum-based composites to extend the relatively limited gypsum application possibilities in the construction industry. The study investigates the use of expanded polystyrene (EPS) beads as an aggregate in gypsum composites, focusing on the printability of the mixture and hardened state mechanical properties in various print directions. Mechanical tests reveal that 3D printing can reduce the compressive strength of the EPS–gypsum composite by between 3% and 32%, and the flexural strength by up to 22%, depending on testing direction. However, the technology opens up new production possibilities for applications where such strength can be sufficient. The study describes that a slight increase in the water-to-gypsum (W/G) ratio in 3D-printed mortars enhances homogeneity and reduces porosity, resulting in improved structural uniformity and therefore higher flexural and compressive strength values. Furthermore, the paper discusses the mechanical anisotropy observed in 3D-printed samples. The combination of 3D printing technology and lightweight gypsum offers the potential for sustainable construction practices by reusing waste materials and creating lightweight, thermally and acoustically insulative, as well as architecturally diverse building components.

**Keywords:** 3D printing; lightweight; waste materials; EPS–gypsum; mechanical properties



**Citation:** Bumanis, G.; Sapata, A.; Sinka, M.; Spurina, E.; Bajare, D. Additive Manufacturing of Lightweight Gypsum and Expanded Polystyrene Granulate Composite. *J. Compos. Sci.* **2023**, *7*, 425. <https://doi.org/10.3390/jcs7100425>

Academic Editor: Francesco Tornabene

Received: 20 August 2023  
Revised: 15 September 2023  
Accepted: 28 September 2023  
Published: 10 October 2023



**Copyright:** © 2023 by the authors. Licensee MDPI, Basel, Switzerland. This article is an open access article distributed under the terms and conditions of the Creative Commons Attribution (CC BY) license (<https://creativecommons.org/licenses/by/4.0/>).

## 1. Introduction

Compared to conventional concrete placement methods, additive manufacturing by 3D printing can reduce material use by 30–60%, significantly cut construction waste, labor costs, and construction-related accidents, and increase building speed by 50–80% [1]. It also allows great freedom for the architectural design and creation of optimized geometric forms [2]. Due to its many advantages, 3D printing is becoming more common in the construction industry nowadays; therefore, it is vital to explore new building materials suited for use in this process.

Gypsum can be considered one of the most ecological binders for several reasons. For example, the energy required for its production is significantly lower than the energy demanded for the production of cement. Calcined gypsum can also be produced not just from natural gypsum rock, but also from industrial waste materials. Furthermore, hardened gypsum can be nearly infinitely recycled into gypsum binder [3].

The combination of 3D printing technology with lightweight materials could be especially suitable for the production of lightweight building elements such as acoustic walls, sandwich panels, lightweight partition walls, vacuum insulated panels (VIPs), and

structural insulated panels (SIPs) due to their merits of high insulation capacity, airtightness, and ease of installation in buildings.

Some studies have researched the printability of lightweight aggregate concrete using aggregates such as expanded clay [3], expanded glass granulate [4], lightweight ceramsite sand [5,6] expanded perlite aggregate [7], and expanded thermoplastic microspheres [8]. During the last decade, research on the development of lightweight gypsum composites as a more environmentally friendly alternative to lightweight cement-based materials has been emerging [9–11], extending the relatively limited gypsum application possibilities. The use of lightweight gypsum composites offers possibilities to create building elements with reduced dead load, improved thermal and acoustic insulation properties, and enhanced fire resistance which contributes to the longer lifespan of constructions [9]. The construction, transportation, and placement costs are lower for lightweight products as well [9,12]. However, studies on the preparation and manufacturing of lightweight gypsum structures by extrusion-based 3D printing are still lacking.

There are two common methods to obtain lightweight gypsum: by adding either a foaming agent or lightweight aggregates.

In the case of adding a foaming agent, a uniform porous structure can be developed in hardened gypsum. The disadvantage of such foaming techniques is the risk of foam collapse due to the pore merging and air release. The aforementioned risk increases as the processing and handling time of the material increases, and 3D printing technology usually requires extra time to deliver material layer-by-layer. The foaming process also reduces material bulk density and mechanical strength [13]. A lightweight aggregate system is more stable but often results in higher density. The use of lightweight aggregates such as expanded vermiculite, diatomite, and expanded granules can be used for the improvement of thermal and sound isolation [14]. Some studies recently have researched how the incorporation of industrial by-products, such as coal fly ash [9], paper pulp waste [15], leather scraps [16], expanded polystyrene (EPS) balls [15,17,18], and others can improve the thermal, mechanical, and acoustic properties of gypsum plaster.

EPS is a nonbiodegradable plastic that is amongst the commodity polymers most produced in the world in order to fulfill the needs of the construction and packing industry. The consumption of EPS continues to increase annually [19]. When using EPS beads as aggregate for gypsum composites, a poor interface between the binder and EPS is formed due to the hydrophobic nature of EPS particles. As a result, not only the mechanical strength and physical properties but the printability of the composite could be affected as well. Hence, effective modifications should be taken to improve the hydrophilicity of EPS particles when used for the preparation of lightweight gypsum [20]. It must be noted that due to the high water absorption ratio, EPS–gypsum composite materials are not suitable for exterior surfaces.

Multiple manufacturing methods can be used for lightweight gypsum composites. The traditional mixing and casting method can be used to incorporate gypsum composite into molds; however, in this case, a flowable material is required. Another technology is associated with cement screed technology, where a semi-dry mixture is prepared using aggregate and binder which can be placed in the floor or molds. By using this technology, a highly lightweight material with a density from 50 to 200 kg/m<sup>3</sup> can be obtained [11]. Similar technology is used in construction sites using Portland cement as a binder. In this manuscript, a third casting method is represented using a 3D printer.

This research focuses on developing a 3D-printable material by finding the most suitable ratio of EPS, gypsum binder, setting retarder, and water for the mix. Mechanical properties in different print directions and in relation to reference samples are investigated as well. Hopefully, the results obtained from the current study will enable us to draw some conclusions on how to extend the application possibilities of lightweight gypsum.

## 2. Materials and Methods

### 2.1. Materials

Gypsum *Baugips* (Knauf, Saurieši, Latvia) was used as binder. The raw gypsum's initial setting time was ~17 min, and the final setting time was ~30 min. As aggregate, recycled EPS beads with a particle size of up to 5 mm were used (GoGridas, Jaunolaine, Latvia). For the specific particle size distribution range of the used EPS beads, see the authors' previous research paper [10], Figure 1, EPS10. A citric acid-based setting retarder, Gips Retard (TKK, Srpenica, Slovenia), was used to slow down the setting time.

### 2.2. Mixture Compositions

Several mixture compositions with different water-to-gypsum (W/G) ratios (see Table 1. Ref-1, Ref-2) and amounts of added gypsum retarder (see Table 1, GR-1, GR-2, GR-3) were tested to further evaluate their suitability for 3D printing.

**Table 1.** Gypsum–EPS mix proportions, g.

Mix	EPS	Baugips	Tap Water	Set Retarder	W/G
Ref-1	10	600	360	-	0.60
Ref-2	10	600	300	-	0.50
GR-1	10	600	300	0.1% (0.6 g)	0.50
GR-2	10	600	300	0.2% (1.2 g)	0.50
GR-4	10	600	300	0.4% (2.4 g)	0.50

### 2.3. Evaluation of Material's Suitability for 3D Printing

From initial research, it was determined that a castable gypsum–EPS composite was obtained by using a ratio of W/G 0.6, which was then used as reference mix Ref-1 (see Table 1). However, when mixing Ref-1, it was found that the W/G ratio should be reduced due to separation of the gypsum paste from the granules (see Figure 1a). By reducing the W/G ratio to 0.5, a homogeneous composite mass was obtained (Mix Ref-2, see Table 1 and Figure 1b). Then, a mixture with a setting time suitable for 3D printing was found by adding a retarder of 0.1% to 0.4% of gypsum mass (see Table 1).



**Figure 1.** Consistency of gypsum–EPS mixtures with different W/G ratios (a) Mixture Ref-1 with W/G = 0.6; (b) Mixture Ref-2 with W/G = 0.5.

Fresh state properties, such as setting time and consistency, were tested. Initial and final setting times were measured using the Vicat apparatus according to BS EN 196-3. The consistency of mixtures was measured using the flow table according to EN 1015-3. The obtained measurements allowed us to evaluate the fluidity and workability of each mixture.

The recorded initial setting time for Ref-1 and Ref-2 was 11 min, which is not suitable for 3D printing. By adding 0.1% setting retarder, the initial setting time increased to 30 min, while 0.2% increased the time to 63 min, and 0.4% increased the time to 90 min, respectively (see Figure 2), which is preferable for 3D printing.

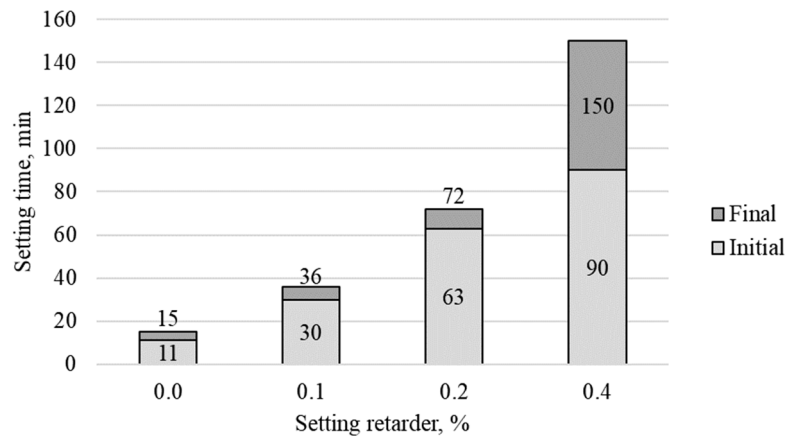


**Figure 2.** Increase in initial and final setting times in relation to added amount of setting retarder.

The spread diameter of each mixture was measured after mixing and close to the beginning of the initial setting time (see Figure 2 and Table 2): at 25 min for GR-1, and at 55 min for GR-2 and GR-4. The addition of setting retarder also ensured that the workability did not change during the open time. It was observed that it is possible to slow down the initial setting time by using gypsum retarder without significantly changing the consistency of the gypsum composite.

**Table 2.** Setting time and consistency of EPS–gypsum composite mixtures.

Mix	Time Recorded, min	Obtained Shape	Obtained Shape after 15 Jolts	Spread Diameter, mm
Ref-1	5			190
Ref-2	5			160

Table 2. Cont.

Mix	Time Recorded, min	Obtained Shape	Obtained Shape after 15 Jolts	Spread Diameter, mm
GR-1	25			168
GR-2	55			150
GR-4	55			170

Mixture GR-2 with 0.2% added retarder showed fresh state properties most suitable for 3D printing; therefore, 3D printing and the following mechanical tests were carried out using this mix.

Three-dimensional printing was carried out twice. In order to achieve the same consistency as for mixture GR-2 (see Table 2), both times the W/G ratio had to be modified. The need for modifications in water amount is a common problem when creating gypsum composite mixtures. It can be explained by different external conditions, such as temperature and relative humidity rates. It must also be noted that the need for technologically free water can decrease due to volume increase. The W/G ratio can be dependent on the dry gypsum batch number and manufacturing date as well. As a result, two additional series of mixtures were created, GR-2b and GR-2c (see Table 3).

Table 3. EPS–gypsum composite mix proportions, g.

Mix	EPS	Baugips	H <sub>2</sub> O	Setting Retarder	W/G	RH, %	Temperature, °C	Notes
GR-2	10	600	300	1.2	0.50	40	22	1 L mixed
GR-2b	10	600	258	1.2	0.43	60	22	12 L mixed
GR-2c	10	600	308	1.2	0.51	50	22	18 L mixed

#### 2.4. Mixing and 3D Printing

First, the setting retarder was added to gypsum and homogenized by mixing and shaking. Second, the gypsum–retarder mixture was mixed with water for 30 s. Then, EPS granules were added and the composite was mixed for an additional 90 s. Mixing was carried out using a portable mortar mixer RUBIMIX-9N with a speed of 780 RPM.

Afterward, the mixture was loaded into the printer. Printing was performed with a custom-made gantry-type printer with batch-type printhead developed within RTU for the printing of concrete and other building materials. The printer frame allows for print region dimensions of  $1500 \times 1000 \times 1000$  mm. For more information on the used printer see [21], while video of the printing can be seen in Video S1.

Before creating any print object, three straight lines were printed using the obtained composite mix GR-2b in order to determine the optimal extrusion speed (see Figure 3a). It was observed that with lower extrusion rates, the mass was on the verge of plasticity, leading to ruptured layer surface formation during the printing process.



**Figure 3.** (a) Material flow with different extrusion rates; (b) Formation of GR-2b composite layers with a 3D printer.

When the optimal extrusion speed was determined, linear and rectangular objects consisting of four layers (see Figure 3b) were printed and samples were also molded. The model can be seen in Figure S1.

A similar mixing and printing procedure was repeated during the secondary printing using composite mix GR-2c. A rectangular print object consisting of four layers was created and samples were molded as well (see Figure 4a,b). Compared to the primary printing, a 50% higher extrusion rate was applied to produce a more homogeneous sample.

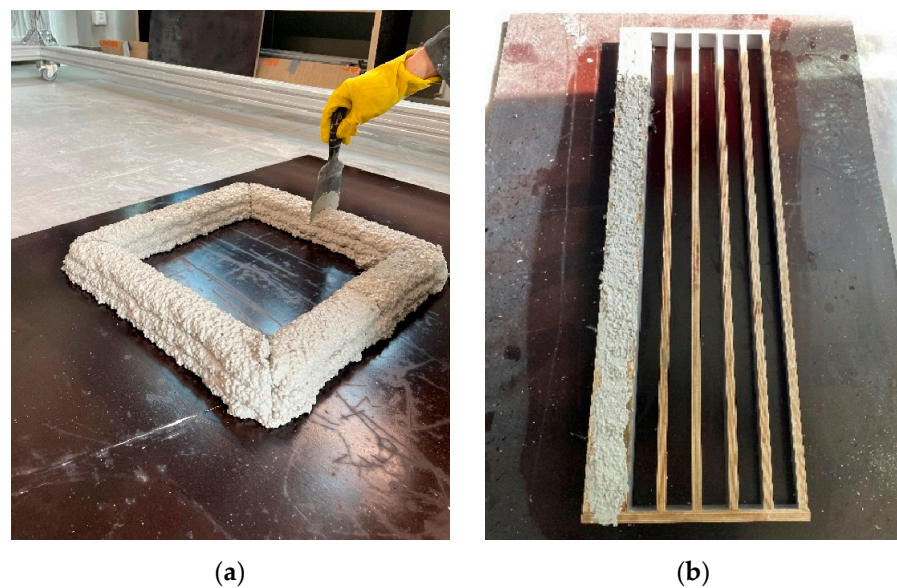


**Figure 4.** (a) Formation of GR-2c composite layers with a 3D printer; (b) Molded samples.

### 2.5. Sample Preparation

The test specimen orientations and coordinate system ( $u, v, w$ ) are defined according to Mechtcherine et al. [22]. In this coordinate system,  $u$  is the direction of the print path,

v is perpendicular to u in the print plane, and w is perpendicular to the print plane. The specimen orientations are named as follows. The first letter indicates the load direction for a normal force (in compressive strength tests) or an axis of rotation for a bending load (in flexural strength tests). The second letter indicates the longitudinal axis of the specimen, used only for prismatic samples in flexural strength tests.

Prior testing, the samples were cut using a circular saw and then marked. When marking the samples, the following symbols were used for each plane: an arrow for the u,w face (indicating the print direction), a cross mark for the v,w face, and a dot for the u,v face (see Figure 5).

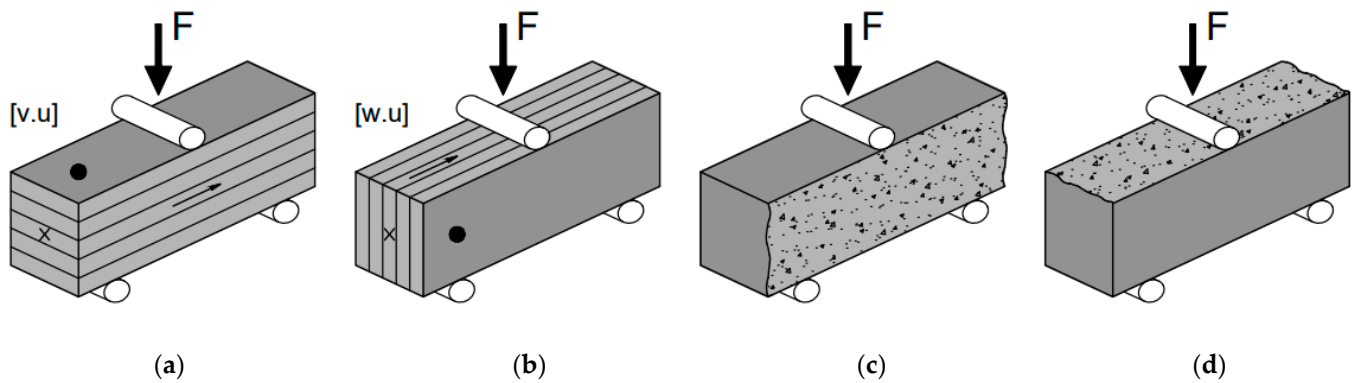


**Figure 5.** Three-point flexural strength test setup and sample orientation: (a) 3D-printed samples, orientation [v.u]; (b) 3D-printed samples, orientation [w.u]; (c) Cast samples, standard orientation; (d) Cast samples, rotated.

Samples were tested after the curing period, at the age of 7 days. Mechanical properties, as well as density, were determined for both printed and cast samples. Flexural strength tests were carried out under three-point loading as per set-up (see Figure 5). Testing was performed in two sets: primary and secondary.

The primary strength tests were carried out using samples made of mixture GR-2b. Printed samples were tested in [v.u] direction (see Figure 5a) during the flexural strength tests and in [w] direction (see Figure 6a) during the compressive strength tests. Cast samples were tested in a standard direction (see Figures 5c and 6c).

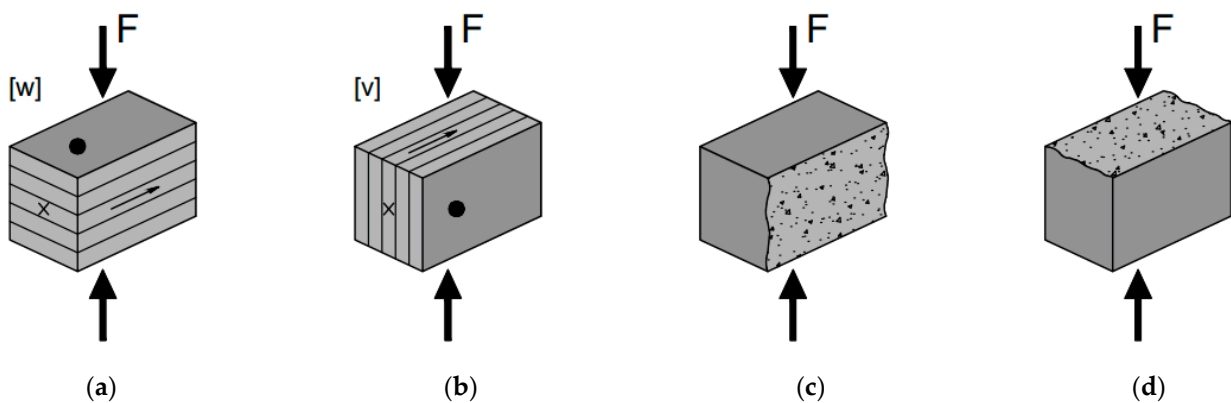


**Figure 6.** Compressive strength test setup and applied compression load perpendicular to top plane: (a) 3D-printed samples, orientation [w]; (b) 3D-printed samples, orientation [v]; (c) Cast samples, standard orientation; (d) Cast samples, rotated.

The secondary strength tests were carried out using samples made of mixture GR-2c. In this case, the samples were tested in directions [v.u] and [w.u] (see Figure 5a,b) during the flexural strength tests. During the compressive strength tests the samples were tested in

directions [w] and [v] (see Figure 6a,b). The secondary test was carried out with cast samples in two different directions as well: standard and rotated (see Figures 5c,d and 6c,d).

It must be noted that the test samples were prepared differently for the primary and secondary tests.

For the primary flexural strength tests, prismatic-shaped elements were cut out of the print object. Side, upper, and top planes remained with the geometry obtained while printing, without further processing by cutting or grinding them (see Figure 7a,c). For the compressive strength tests, cubes were cut out of the print object (see Figure 7b).

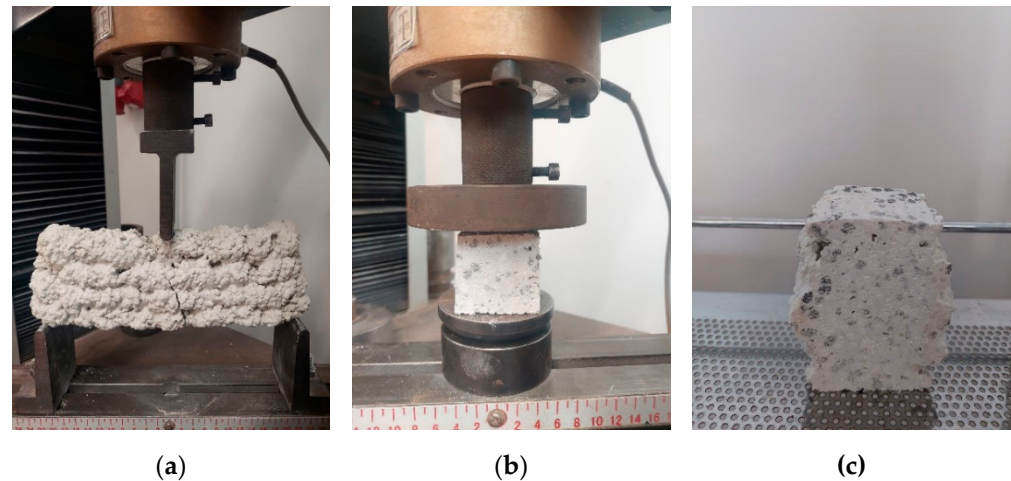


**Figure 7.** Primary testing of 3D-printed samples: (a) Flexural strength test in [v.u] direction; (b) Compressive strength test in [v] direction; (c) Cross section of 3D-printed sample.

For the secondary flexural strength tests, printed samples were cut using a circular saw in order to achieve a regular prismatic shape (see Figure 8a,b). Secondary compressive strength tests were carried out using the broken halves of prisms used in the flexural strength test.

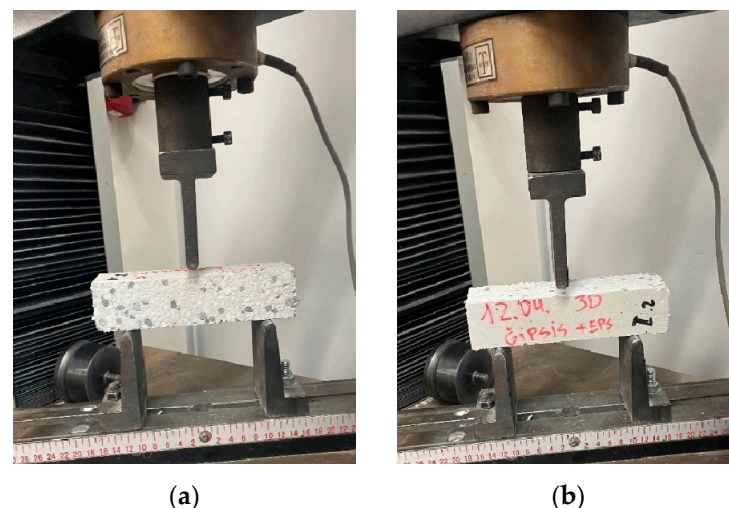


**Figure 8.** Secondary testing of 3D-printed samples: (a) Flexural strength test in [v.u] direction; (b) Flexural strength test in [w.u] direction.

### 3. Results and Discussion

#### 3.1. Fresh State Properties

Setting time and consistency were tested for the printed composite mixtures and recorded in Table 4. The flow of the mixture was measured before loading in the 3D printer,

14 and 38 min after mixing. The mix had a slump of 138 mm after 38 min, indicating a sufficient open time for 3D printing. The consistency remained practically unchanged during the test period.

**Table 4.** Setting time and consistency of 3D-printed EPS–gypsum composite mixture GR2-b.

Property	Time, min	Obtained Shape and Spread Diameter, mm
After lifting the cone	0	
After 15 jolts	14	
After 25 jolts	38	
Flow	14	140 × 140
	38	140 × 135
Initial setting time	-	50 min
Fresh density	-	950 kg/m <sup>3</sup>

### 3.2. Mechanical Properties

The fresh state density of the GR-2b mix was 950 kg/m<sup>3</sup>. After 3D printing and curing, the mean density of the samples was 643 kg/m<sup>3</sup>, compared to 741 kg/m<sup>3</sup> for the cast samples (see Figure 9). Three-dimensional printing reduced the density as well as the flexural and compressive strength of the EPS–gypsum composite mix.

Three-dimensional-printed samples tested in the [v.u] direction reached 52% of cast sample flexural strength. It must be noted that the non-homogenous cross-sections of the printed samples might be the reason behind the relatively high standard deviation values. The mean compressive strength results showed that 3D-printed samples tested in the [w] direction reached 64% of the cast sample strength.

Secondary test results: the fresh state density of the GR-2c mix was 1107 kg/m<sup>3</sup>. After 3D printing and curing, the mean density of samples was 726 kg/m<sup>3</sup>, and 637 kg/m<sup>3</sup> for cast samples (see Figure 10).

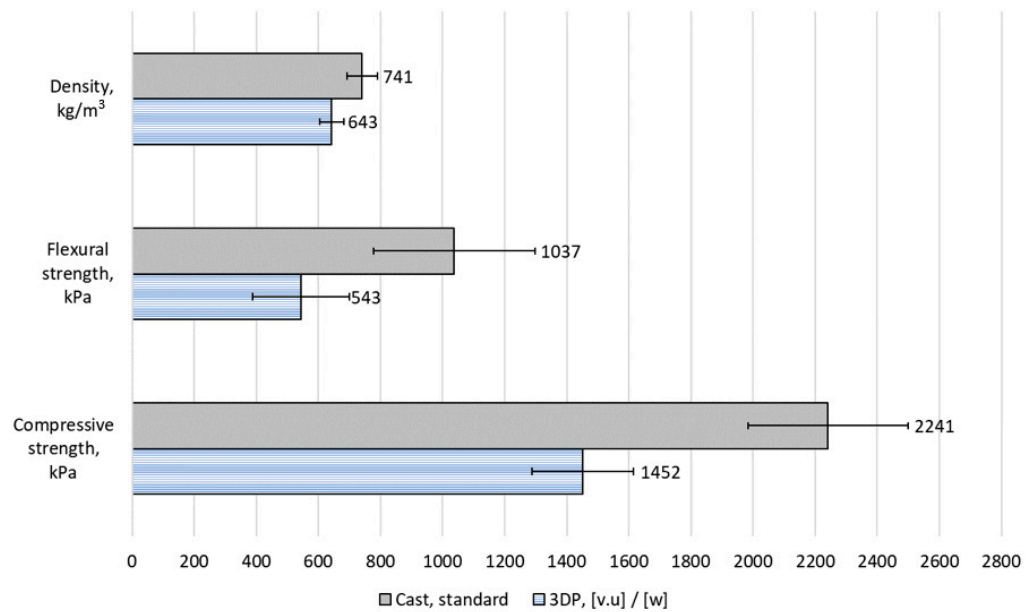


**Figure 9.** Primary test results: density (kg/m<sup>3</sup>), flexural and compressive strength (kPa) of cast and 3D-printed samples.

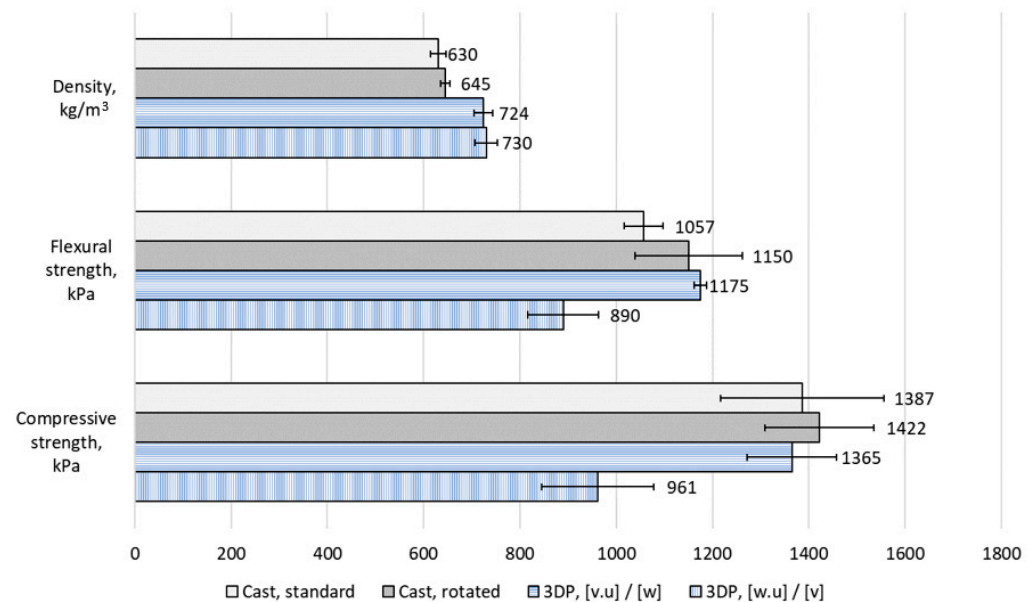


**Figure 10.** Secondary test results: density (kg/m<sup>3</sup>), flexural and compressive strength (kPa) of cast and 3D-printed samples.

When comparing test results of cast samples tested in different directions, no significant differences were observed. This indicates that the EPS beads do not exhibit any tendency to align in a specific direction, and there is no segregation of the fresh mixture during the molding process.

Test results revealed negligibly higher (6%) flexural strength values for 3DP samples tested in the [v.u] direction compared to the cast samples. However, 3DP samples tested in the [w.u] direction reached only 78% of the average flexural strength of cast samples.

A similar trend was observed with the compressive strength results. Significantly higher values were recorded when applying the load perpendicular to the print direction. Samples tested in the [w] direction reached 97% of the average cast sample strength. However, compressive strength was noticeably lower for the [v] direction, reaching only 68% of the average cast sample strength.

In traditional mortar manufacturing methods, one of the primary factors contributing to achieving high density and mechanical properties is maintaining a low water-to-binder ratio. This can also be observed in our study where mortars with two different W/G ratios were cast in molds. As expected, the lower W/G ratio correlated with higher cast sample density and compressive strength, as indicated in Table 5.

**Table 5.** Primary test result comparison with secondary test results.

	Density		Flexural Strength		Compressive Strength	
	GR-2b W/G = 0.43	GR-2c W/G = 0.51	GR-2b W/G = 0.43	GR-2c W/G = 0.51	GR-2b W/G = 0.43	GR-2c W/G = 0.51
Cast	741	638	1037	1104	2241	1405
3DP [v.u]/[w]	643	724	543	1175	1452	1365

However, when the mortar is 3D printed, other mechanisms can affect the final results. Three-dimensional-printed mortars typically lack compaction post material deposition, which leads to the formation of air voids, inhomogeneity, and mechanical anisotropy [22]. In this study, the mixture GR-2c with a higher ratio of W/G was used for the secondary printing in comparison with the mixture GR-2b used for the primary printing. Consequently, the GR-2c mixture’s consistency was more homogeneous and possessed improved printability (see Figures 3b and 4a). As a result, the hardened test samples from mixture GR-2c contained fewer pores and caverns, resulting in higher structural uniformity, which might be the reason behind the higher density and flexural strength despite the higher W/G ratio (see Table 5). Similar observations have been reported by other researchers in their studies [23,24].

From the results presented in Figure 10, it can be seen that bulk density does not correlate well with the mechanical strength results of 3D-printed samples in different directions, which indicates that mechanical strength is influenced by other mechanisms.

Samples tested in direction [v] showed lower compressive strength than samples tested in [w] direction. Similar patterns were observed by Panda et al. [25], Sanjayan et al. [26], and Nerella et al. [27]. Their explanation was that without any mold or formwork, fresh 3D-printed mortar is free to expand laterally due to the self-weight of the concrete. As a result, the lateral direction is the least compacted direction during the setting process and therefore the weakest.

The degree of concrete compaction may have played a significant role in the flexural strength test results as well. The flexural strength is usually determined by the central bottom area of specimens where the maximum tensile stress occurs [25]. The compaction due to self-weight occurs on the bottom layer more than the top ones. This phenomenon results in higher load capacity of the bottom layer, which could be the explanation behind the higher flexural strength in direction [v.u] in comparison with direction [w.u].

It is generally acknowledged that the existence of interlayers also causes mechanical anisotropy of 3D-printed concrete and mortars. When the surface of the bottom layer is exposed to the air, it becomes drier and absorbs moisture from the fresh upper layer, creating a continuous void structure, causing insufficient hydration reaction and the formation of entrapped air at the interlayer, which leads to weak interlayer bonding strength [28,29]. However, existing research [22,27,29] shows that neither flexural tests performed in directions [v.u] or [w.u], nor compression tests performed in any direction, can provide exact data on interfacial bond strength. Other tests, such as tensile loading, pull-off tests, or flexural tensile strength tests, where the force is applied to the interface plane, would be more suitable. Hence, it is highly likely that interlayer bond strength has minimal influence on the mechanical anisotropy observed in this study.

### 3.3. Three-Dimensional Printing Buildability and Quality

The quality of 3D-printed element geometry was evaluated by two factors. First, changes in total print object length with each added layer (see Figures 11 and S2a) were measured. Second, changes in print object cross-section width were measured (see Figure 11a,b).

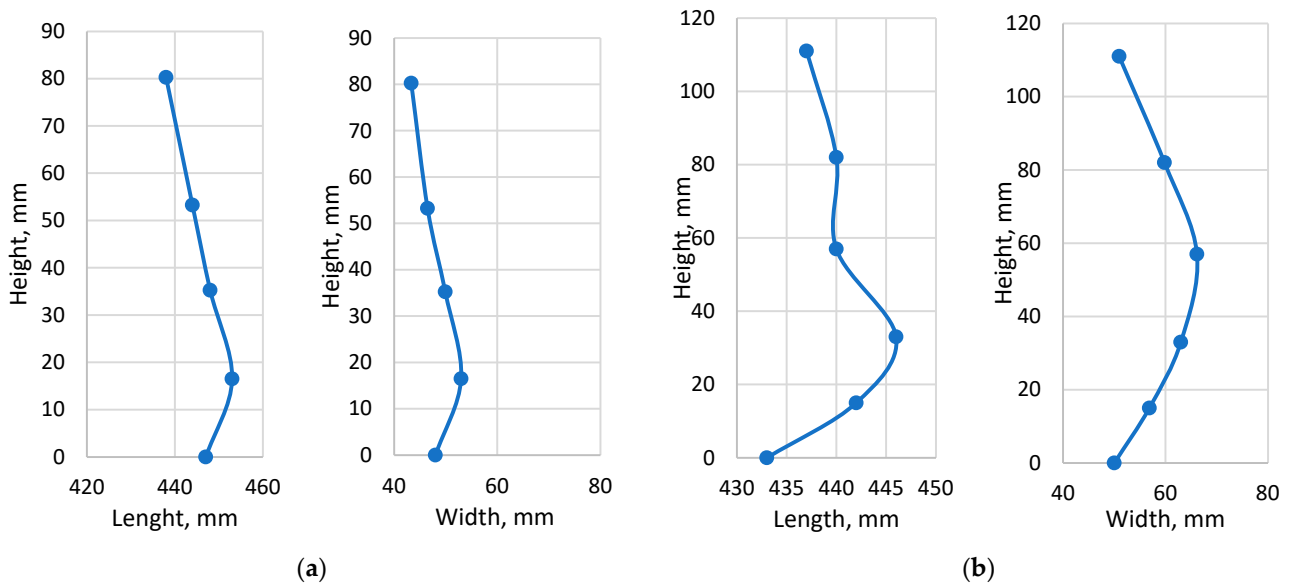


**Figure 11.** Length and width measurements of 3D-printed objects with (a) rectangular shape; (b) linear shape.

As shown in Figure 11, changes in total print object length are affected by the printed element shape (rectangular or linear). Due to restraints and support given by rectangular-shaped print object corners, layers with more evenly distributed lengths can be achieved in comparison with print objects with a linear shape. The setting of the bottom layers was observed in both cases.

In Figure S2b, the cross-section measurements of prismatic-shaped specimens are given. The printed specimen cross-section width ranges from 56.0 to 63.8 mm. As previously described, the force applied by the nozzle to compress every new layer can be associated with the reduced width of the last layer [30]. Therefore, the pre-compression extruded layer shape and the post-compression extruded layer shape can be separated. The overall homogeneity of post-compression layers varies from 88% to 91% for rectangular print. The boundary between the two following layers is with the reduced width, as previously it was observed for 3D-printed cement mortar [31].

## 4. Conclusions

The EPS–gypsum composite mixtures with the obtained fresh-state properties are suitable for 3D printing. However, further research is necessary in order to test its buildability, as well as enhance its rheological properties.

In the fresh state, the EPS beads did not exhibit a tendency to align in a certain direction during the molding process. However, a tendency for aggregates to line in the print direction was observed in the 3D-printed samples.

In this study, increasing the W/G ratio of the mixture improved printability, reduced porosity, and enhanced the overall structural uniformity of the final samples. Consequently, this led to higher flexural and compressive strength values.

In various test directions, the samples exhibited significantly different compressive and flexural strength values. The observed mechanical anisotropy in this study, especially when assessing sample flexural strength in the [v.u] and [w.u] directions, can most likely be attributed to variations in the compaction degree.

The obtained EPS–gypsum composite material has a relatively low mechanical strength, and the 3D printing process can reduce it even further. However, when developing lightweight composites, the primary concern is not always achieving high mechanical properties, but rather ensuring that these properties are sufficient to support the self-weight of the final structure. Hence, the most effective approach to utilize the advantages of lightweight gypsum composites is to combine them with load-bearing structures. Additionally, the combination of 3D printing technology with lightweight materials, particularly gypsum-based composites, offers the construction industry a promising avenue for producing lightweight building elements with enhanced properties and reduced environmental impact. The production of highly efficient sound-absorbing walls, where both the porous structure of the material and the textured surface of the 3D-printed element contribute to the sound-absorbing qualities, could be made more straightforward. Moreover, this combination could simplify the process of producing permanent molds with insulation properties for bearing concrete constructions. Three-dimensional printing is a relatively automated and easily repeatable process that enables the production of elements with consistent quality. Overall, the combination of EPS–gypsum composites with 3D printing technology would not only allow the reuse of construction waste but would combine the insulating and lightweight properties of EPS with possibilities of automation and the creation of free architectural forms offered by additive manufacturing as well.

Further research should be carried out to gain insight into the physical properties of EPS–gypsum composite, such as thermal and acoustic conductivity, water absorption, and fire resistance in order to evaluate the most suitable application for this material.

**Supplementary Materials:** The following supporting information can be downloaded at: <https://www.mdpi.com/article/10.3390/jcs7100425/s1>, Figure S1: Print path of the printed elements; Figure S2: (a) Measurements of 3D-printed object layer height and cross-section width; (b) Measurement of 3D-printed EPS–gypsum sample cross-section. The following supporting information can be seen at: <https://www.youtube.com/watch?v=Ax7Uq8TeNoM> (accessed on 28 September 2023), Video S1: 3D printing with gypsum + EPS first trial.

**Author Contributions:** Conceptualization, G.B. and M.S.; methodology, G.B. and M.S.; software, M.S.; validation, G.B. and M.S.; formal analysis, G.B., E.S. and M.S.; investigation, G.B., A.S., E.S. and M.S.; resources, M.S. and D.B.; data curation, G.B., A.S. and E.S.; writing—original draft preparation, A.S.; writing—review and editing, G.B., A.S. and M.S.; visualization, G.B., A.S. and M.S.; supervision, G.B., M.S. and D.B.; project administration, D.B.; funding acquisition, D.B. All authors have read and agreed to the published version of the manuscript.

**Funding:** This research was funded by the FLPPs (Fundamental and Applied Research Projects) Program in Latvia under the research project lzp-2020/1-0010: Reuse of gypsum and expanded polymers from construction and demolition waste for acoustic and thermal insulation panels.

**Data Availability Statement:** Data are available on request due to project privacy restrictions.

**Conflicts of Interest:** The authors declare no conflict of interest.

## References

1. Craveiro, F.; Nazarian, S.; Bartolo, H.; Bartolo, P.J.; Pinto Duarte, J. An Automated System for 3D Printing Functionally Graded Concrete-Based Materials. *Addit. Manuf.* **2020**, *33*, 101146. [[CrossRef](#)]
2. Zhang, Y.; Zhang, Y.; She, W.; Yang, L.; Liu, G.; Yang, Y. Rheological and Harden Properties of the High-Thixotropy 3D Printing Concrete. *Constr. Build. Mater.* **2019**, *201*, 278–285. [[CrossRef](#)]
3. Rahul, A.V.; Santhanam, M. Evaluating the Printability of Concretes Containing Lightweight Coarse Aggregates. *Cem. Concr. Compos.* **2020**, *109*, 103570. [[CrossRef](#)]
4. Matthäus, C.; Back, D.; Weger, D.; Kränkel, T.; Scheydt, J.; Gehlen, C. Effect of Cement Type and Limestone Powder Content on Extrudability of Lightweight Concrete. In Proceedings of the Second RILEM International Conference on Concrete and Digital Fabrication: Digital Concrete 2020, online, 6–9 July 2020.
5. Wang, L.; Jiang, H.; Li, Z.; Ma, G. Mechanical Behaviors of 3D Printed Lightweight Concrete Structure with Hollow Section. *Arch. Civ. Mech. Eng.* **2020**, *20*, 16. [[CrossRef](#)]
6. Deng, Z.; Jia, Z.; Zhang, C.; Wang, Z.; Jia, L.; Ma, L.; Wang, X.; Zhang, Y. 3D Printing Lightweight Aggregate Concrete Prepared with Shell-Packing-Aggregate Method-Printability, Mechanical Properties and Pore Structure. *J. Build. Eng.* **2022**, *62*, 105404. [[CrossRef](#)]

7. Mohammad, M.; Masad, E.; Seers, T.; Al-Ghamdi, S.G. High-Performance Light-Weight Concrete for 3D Printing. In Proceedings of the Second RILEM International Conference on Concrete and Digital Fabrication: Digital Concrete 2020, online, 6–9 July 2020; pp. 459–467.
8. Cuevas, K.; Strzałkowski, J.; Kim, J.S.; Ehm, C.; Glotz, T.; Chougan, M.; Ghaffar, S.H.; Stephan, D.; Sikora, P. Towards Development of Sustainable Lightweight 3D Printed Wall Building Envelopes—Experimental and Numerical Studies. *Case Stud. Constr. Mater.* **2023**, *18*, e01945. [[CrossRef](#)]
9. Charai, M.; Mghazli, M.O.; Channouf, S.; El hammouti, A.; Jagadesh, P.; Moga, L.; Mezrhab, A. Lightweight Waste-Based Gypsum Composites for Building Temperature and Moisture Control Using Coal Fly Ash and Plant Fibers. *Constr. Build. Mater.* **2023**, *393*, 132092. [[CrossRef](#)]
10. Argalis, P.P.; Bumanis, G.; Bajare, D. Gypsum Composites with Modified Waste Expanded Polystyrene. *J. Compos. Sci.* **2023**, *7*, 203. [[CrossRef](#)]
11. Bumanis, G.; Argalis, P.P.; Sahmenko, G.; Mironovs, D.; Rucevskis, S.; Korjakins, A.; Bajare, D. Thermal and Sound Insulation Properties of Recycled Expanded Polystyrene Granule and Gypsum Composites. *Recycling* **2023**, *8*, 19. [[CrossRef](#)]
12. Doleželová, M.; Scheinherrová, L.; Krejšová, J.; Keppert, M.; Černý, R.; Vimmrová, A. Investigation of Gypsum Composites with Different Lightweight Fillers. *Constr. Build. Mater.* **2021**, *297*, 123791. [[CrossRef](#)]
13. Çolak, A. Density and Strength Characteristics of Foamed Gypsum. *Cem. Concr. Compos.* **2000**, *22*, 193–200. [[CrossRef](#)]
14. Gencil, O.; del Coz Diaz, J.J.; Sutcu, M.; Koksall, F.; Rabanal, F.P.Á.; Martínez-Barrera, G. A Novel Lightweight Gypsum Composite with Diatomite and Polypropylene Fibers. *Constr. Build. Mater.* **2016**, *113*, 732–740. [[CrossRef](#)]
15. Balti, S.; Boudenne, A.; Dammak, L.; Hamdi, N. Mechanical and Thermophysical Characterization of Gypsum Composites Reinforced by Different Wastes for Green Building Applications. *Constr. Build. Mater.* **2023**, *372*, 130840. [[CrossRef](#)]
16. Ding, X.; Wang, S.; Dai, R.; Chen, H.; Shan, Z. Hydrogel Beads Derived from Chrome Leather Scraps for the Preparation of Lightweight Gypsum. *Environ. Technol. Innov.* **2022**, *25*, 102224. [[CrossRef](#)]
17. Bouzit, S.; Merli, F.; Sonebi, M.; Buratti, C.; Taha, M. Gypsum-Plasters Mixed with Polystyrene Balls for Building Insulation: Experimental Characterization and Energy Performance. *Constr. Build. Mater.* **2021**, *283*, 122625. [[CrossRef](#)]
18. Bicer, A.; Kar, F. Thermal and Mechanical Properties of Gypsum Plaster Mixed with Expanded Polystyrene and Tragacanth. *Therm. Sci. Eng. Prog.* **2017**, *1*, 59–65. [[CrossRef](#)]
19. San-Antonio-González, A.; Merino, M.D.R.; Arrebola, C.V.; Villoria-Sáez, P. Lightweight Material Made with Gypsum and EPS Waste with Enhanced Mechanical Strength. *J. Mater. Civ. Eng.* **2016**, *28*, 04015101. [[CrossRef](#)]
20. Jin, Z.; Ma, B.; Su, Y.; Qi, H.; Lu, W.; Zhang, T. Preparation of Eco-Friendly Lightweight Gypsum: Use of Beta-Hemihydrate Phosphogypsum and Expanded Polystyrene Particles. *Constr. Build. Mater.* **2021**, *297*, 123837. [[CrossRef](#)]
21. Spurina, E.; Sinka, M.; Ziemelis, K.; Vanags, A.; Bajare, D. The Effects of Air-Entraining Agent on Fresh and Hardened Properties of 3D Concrete. *J. Compos. Sci.* **2022**, *6*, 281. [[CrossRef](#)]
22. Mechtcherine, V.; van Tittelboom, K.; Kazemian, A.; Kreiger, E.; Nematollahi, B.; Nerella, V.N.; Santhanam, M.; de Schutter, G.; Van Zijl, G.; Lowke, D.; et al. A Roadmap for Quality Control of Hardening and Hardened Printed Concrete. *Cem. Concr. Res.* **2022**, *157*, 106800. [[CrossRef](#)]
23. Liu, X.; Li, Q.; Wang, L.; Wang, F.; Ma, G. Systematic Approach for Printability Evaluation and Mechanical Property Optimization of Spray-Based 3D Printed Mortar. *Cem. Concr. Compos.* **2022**, *133*, 104688. [[CrossRef](#)]
24. Kloft, H.; Krauss, H.-W.; Hack, N.; Herrmann, E.; Neudecker, S.; Varady, P.A.; Lowke, D. Influence of Process Parameters on the Interlayer Bond Strength of Concrete Elements Additive Manufactured by Shotcrete 3D Printing (SC3DP). *Cem. Concr. Res.* **2020**, *134*, 106078. [[CrossRef](#)]
25. Panda, B.; Chandra Paul, S.; Jen Tan, M. Anisotropic Mechanical Performance of 3D Printed Fiber Reinforced Sustainable Construction Material. *Mater. Lett.* **2017**, *209*, 146–149. [[CrossRef](#)]
26. Sanjayan, J.G.; Nematollahi, B.; Xia, M.; Marchment, T. Effect of Surface Moisture on Inter-Layer Strength of 3D Printed Concrete. *Constr. Build. Mater.* **2018**, *172*, 468–475. [[CrossRef](#)]
27. Nerella, V.N.; Hempel, S.; Mechtcherine, V. Effects of Layer-Interface Properties on Mechanical Performance of Concrete Elements Produced by Extrusion-Based 3D-Printing. *Constr. Build. Mater.* **2019**, *205*, 586–601. [[CrossRef](#)]
28. Van Der Putten, J.; Deprez, M.; Cnudde, V.; De Schutter, G.; Van Tittelboom, K. Microstructural Characterization of 3D Printed Cementitious Materials. *Materials* **2019**, *12*, 2993. [[CrossRef](#)]
29. Wang, C.; Chen, B.; Vo, T.L.; Rezania, M. Mechanical Anisotropy, Rheology and Carbon Footprint of 3D Printable Concrete: A Review. *J. Build. Eng.* **2023**, *76*, 107309. [[CrossRef](#)]
30. Shakor, P.; Nejadi, S.; Paul, G. A Study into the Effect of Different Nozzles Shapes and Fibre-Reinforcement in 3D Printed Mortar. *Materials* **2019**, *12*, 1708. [[CrossRef](#)]
31. Cwalina, C.D.; Harrison, K.J.; Wagner, N.J. Rheology of Cubic Particles Suspended in a Newtonian Fluid. *Soft Matter* **2016**, *12*, 4654–4665. [[CrossRef](#)]

**Disclaimer/Publisher's Note:** The statements, opinions and data contained in all publications are solely those of the individual author(s) and contributor(s) and not of MDPI and/or the editor(s). MDPI and/or the editor(s) disclaim responsibility for any injury to people or property resulting from any ideas, methods, instructions or products referred to in the content.